



Contents lists available at ScienceDirect

Journal of Ginseng Research

journal homepage: <http://www.ginsengres.org>

Research Article

The non-saponin fraction of Korean Red Ginseng (KGC05P0) decreases glucose uptake and transport *in vitro* and modulates glucose production via down-regulation of the PI3K/AKT pathway *in vivo*

Soo-Jeung Park¹, Dasom Lee¹, Dakyung Kim¹, Minhee Lee¹, Gyo In², Sung-Tai Han²,
Sung Won Kim², Mi-Hyang Lee², Ok-Kyung Kim^{3,**}, Jeongmin Lee^{1,*}

¹ Department of Medical Nutrition, Kyung Hee University, Yongin, Gwangju, Republic of Korea

² Korea Ginseng Corporation Research Institute, Korea Ginseng Corporation, Daejeon, Gwangju, Republic of Korea

³ Division of Food and Nutrition and Research Institute for Human Ecology, Chonnam National University, Gwangju, Republic of Korea

ARTICLE INFO

Article history:

Received 26 June 2019

Received in Revised form

8 November 2019

Accepted 10 December 2019

Available online 17 December 2019

Keywords:

Diabetes mellitus

Korean Red Ginseng

Non-saponin fraction

Glucose regulation

ABSTRACT

Background: The non-saponin fraction of Korean Red Ginseng has been reported to have many biological activities. However, the effect of this fraction on anti-diabetic activity has not been elucidated in detail. In this study, we investigated the effects of KGC05P0, a non-saponin fraction of Korean Red Ginseng, on anti-diabetic activity *in vitro* and *in vivo*.

Methods: We measured the inhibition of commercially obtained α -glucosidase and α -amylase activities *in vitro* and measured the glucose uptake and transport rate in Caco-2 cells. C57BL/6J mice and C57BLKS/J^{db/db} (diabetic) mice were fed diets with or without KGC05P0 for eight weeks. To perform the experiments, the groups were divided as follows: normal control (C57BL/6J mice), db/db control (C57BLKS/J^{db/db} mice), positive control (inulin 400 mg/kg b.w.), low (KGC05P0 100 mg/kg b.w.), medium (KGC05P0 200 mg/kg b.w.), and high (KGC05P0 400 mg/kg b.w.).

Results: KGC05P0 inhibited α -glucosidase and α -amylase activities *in vitro*, and decreased glucose uptake and transport rate in Caco-2 cells. In addition, KGC05P0 regulated fasting glucose level, glucose tolerance, insulin, HbA1c, carbonyl contents, and proinflammatory cytokines in blood from diabetic mice and significantly reduced urinary glucose excretion levels. Moreover, we found that KGC05P0 regulated glucose production by down-regulation of the PI3K/AKT pathway, which inhibited gluconeogenesis.

Conclusion: Our study thereby demonstrated that KGC05P0 exerted anti-diabetic effects through inhibition of glucose absorption and the PI3K/AKT pathway in *in vitro* and *in vivo* models of diabetes. Our results suggest that KGC05P0 could be developed as a complementary food to help prevent T2DM and its complications.

© 2020 The Korean Society of Ginseng, Published by Elsevier Korea LLC. This is an open access article under the CC BY-NC-ND license (<http://creativecommons.org/licenses/by-nc-nd/4.0/>).

1. Introduction

Diabetes mellitus (DM) is the third most common chronic disease in the world and causes serious complications such as nephropathy, neuropathy, and retinopathy [1,2]. This disease is classified into type I DM, known as childhood diabetes or insulin-dependent type, and type II DM, known as adult diabetes or insulin-dependent type [3]. A number of patients on most diabetes medications have difficulty in maintaining long-term glycemic control and experience adverse effects. Therefore, the development

of natural product-derived substances with insulin-like activity is a promising approach.

One of the characteristics of DM is the change in liver metabolism. The liver plays a very important role in the regulation of systemic metabolism of energy nutrients. When the target tissue for insulin is damaged, insulin resistance occurs because the response function is lowered, and the liver can then no longer control glucose homeostasis [4]. Most of the body's production of glucose occurs in the liver and kidneys, and the liver acutely responds to insulin by reducing the production of glucose [5]. In the

* Corresponding author. Department of Medical Nutrition, Kyung Hee University, Yongin, 17104, Republic of Korea.

** Corresponding author. Division of Food and Nutrition and Research Institute for Human Ecology, Chonnam National University, Gwangju, 61186, Republic of Korea.

E-mail addresses: 20woskxm@jnu.ac.kr (O.-K. Kim), jlee2007@khu.ac.kr (J. Lee).

fed state, insulin binds to its receptor (IR), which then begins phosphorylation of its substrates. This in turn causes the activation of phosphatidylinositol-3-kinase (PI3K) and leads to the phosphorylation of PI3K. This pathway activates protein kinase B (PKB/AKT) and causes the phosphorylation of AKT, which leads to the suppression of phosphoenolpyruvate carboxykinase (PEPCK) and glucose-6-phosphatase (G6Pase), which are known as hepatic gluconeogenic genes [6–8].

The db/db mouse model is the most widely used model for type II DM studies and is characterized by leptin deficiency. Deficiency of leptin secretion in the hypothalamus leads to persistent excess appetite and obesity, resulting in hyperglycemia and abnormalities of renal function [9,10].

Korean Red Ginseng (RG, *Panax ginseng* Meyer) is an herb that has been traditionally used for thousands of years in Asian countries [1]. RG is produced by repeatedly heating and drying the roots of ginseng. It has strong pharmacological effects in several diseases, such as diabetes, cancer, and inflammatory diseases [11–13]. In particular, saponin, which is known to be an active ingredient of red ginseng, showed benefits in studies of diabetes, apoptosis, cardiac damage, and obesity [14–17]. However, there have been few evaluations of the pharmacological activity in diabetes of the non-saponin fraction of Korean Red Ginseng.

In this study, we first investigated whether the non-saponin fraction of Korean Red Ginseng (KGC05P0) inhibits α -glucosidase and α -amylase activities *in vitro*. Second, we assessed the effects of KGC05P0 on glucose uptake and transport rate in Caco-2 cells, and third, we assessed its effects on glycemic control through down-regulation of the PI3K/AKT pathway in diabetic db/db mice.

2. Materials and methods

2.1. Preparation of the non-saponin fraction of Korean Red Ginseng

The non-saponin fraction of Korean Red Ginseng (KGC05P0) was obtained from Korea Ginseng Corporation Research Institute (Daejeon, Korea). This is a powder sample in which only saponin was removed from red ginseng concentrate through non-saponin fractionation procedure. This procedure was carried out after filling Diaion (HP-20, Mitsubishi Chemical Industries, Ltd.) into the fractionation apparatus, adding 80% alcohol, and washing it with purified water until no alcohol remained. The concentrate was diluted to 10% in purified water and then filtered, and water fraction and 30% ethanol fraction were respectively performed. The two fractions were combined, concentrated, and spray dried to complete the sample preparation. KGC05P0 was sealed to protect from air and light and stored at -20°C until use.

2.2. High-performance liquid chromatography (HPLC) analysis

KGC05P0 (1.0 g) was weighted in a 50 mL volumetric flask, and 50 mL of deionized water was added and extracted by an ultrasonic method at room temperature for 30 min. Ethanol (4 mL) was added to the extract solution (1 mL), and the precipitate was collected and diluted with water (10 mL). The solution (0.5 mL) was condensed under air at 60°C . 2M TFA (trifluoroacetic acid, 1 mL) was added to hydrolyze, reacted in an oven at 121°C for 90 min, and then condensed under air at 60°C and PMP derivatization was performed by adding 0.3M NaOH (100 μL) and 0.5M PMP (1-phenyl-3-methyl-5-pyrazolone, 120 μL) for 1 h at 70°C in an oven. After neutralizing with 0.3M HCl (100 μL), the mixture was shaken by adding water (1 mL) and chloroform (1 mL). Then, the solution was injected into the HPLC system after getting the filtered water layer.

HPLC analysis was performed with a Waters alliance performance liquid chromatography instrument (Waters, USA) equipped with a photo diode array detector (Waters, USA). A Discovery C18 column (4.6 mm \times 250 mm, 5 μm particles) was used for separation. The column temperature was 35°C , the flow rate was 1.0 mL/min, and the injection volume was 10 μL . The mobile phase consisted of 0.01M phosphate buffer (pH 6.7) (A) and acetonitrile (B). HPLC gradient conditions were as follows: 0–35 min (15% B), 35–45 min (15–20% B), 45–55 min (20% B), 55–56 min (20–15% B), and 60 min (15% B). The detection wavelength was set at 250 nm.

2.3. Measurement of α -glucosidase and α -amylase inhibitory activities

α -Glucosidase and α -amylase activity colorimetric assay kits were purchased from Biovision (Milpitas Blvd., Milpitas, CA, USA). α -Glucosidase, α -amylase, and acarbose were purchased from Sigma-Aldrich (St. Louis, MO, USA). KGC05P0 (0–2000 $\mu\text{g}/\text{mL}$), inulin (0–2000 $\mu\text{g}/\text{mL}$), and acarbose (1000 $\mu\text{g}/\text{mL}$) were added to 96-well plates. For the α -glucosidase inhibitory activity assay, 10 μL of α -glucosidase (1.0 U/mL) was added to each well, and assay buffer was added for a total volume of 50 $\mu\text{L}/\text{well}$. A volume of 50 μL of reaction mix containing 3 μL of α -glucosidase substrate mix was added to each well, and the absorbance was read with an iMARK™ Microplate Reader (Bio-Rad Laboratories, Hercules, CA, USA) at 410 nm. For the α -amylase inhibitory activity assay, a volume of 5 μL of α -amylase (3 U/mL) was added to each well, and the volume was adjusted to 50 $\mu\text{L}/\text{well}$ with sterile distilled water. A volume of 100 μL of reaction mix containing 50 μL of substrate mix was added to each well, and absorbance readings were recorded at 405 nm. The experiments were conducted according to Bio-Rad's protocol.

2.4. Caco-2 cell culture and glucose transport measurement

The human colon adenocarcinoma cell line (Caco-2) was purchased from the American Type Culture Collection (ATCC, Rockville, MD, USA) and cultured in a 95% air/5% CO_2 atmosphere at 37°C . Cells were grown in DMEM, supplemented with 20% FBS, 1% P/S, 1% sodium pyruvate, and 1% NEAA mixture. The glucose uptake colorimetric assay kit used in the experiment was purchased from Biovision. Cells were seeded into a transwell plate (Corning® Transwell®, 24 mm diameter, pore size 0.4 μm) at a density of 1×10^4 cells/ cm^2 and cultured for 21 days. The electrical resistance of the cell monolayers was measured to confirm that cell differentiation had occurred, and the medium was replaced with serum-free medium 24 h before the permeability study. For the experiment, the medium was discarded, 2 mL of Krebs-Ringer-Phosphate-HEPES (KRPH) buffer (Biosolution Co., Seoul, Korea) containing 2% BSA was added to each well, and the plate was incubated for 40 min at 37°C . After washing, KGC05P0 (0–500 $\mu\text{g}/\text{mL}$) samples were added to the plate, which was then incubated for 3 h at 37°C . A volume of 10 μL of 10mM 2-DG was added to each well, and the plate was incubated for 20 min. After the washing, NADPH generation, NADPH degradation, and recycling amplification reaction steps, the absorbance was read with an iMARK™ Microplate Reader (Bio-Rad) at 412 nm. The experiment was conducted according to Bio-Rad's protocol.

2.5. HepG2 cell culture and treatments

The human hepatocellular carcinoma cell (HepG2) was purchased from ATCC and cultured in a 95% air/5% CO_2 atmosphere at 37°C . HepG2 cells were grown in DMEM, supplemented with 10%

Table 1
Primer sequences used in real-time PCR quantification of mRNA

| Gene | Human sequences | Murine sequences |
|--------|------------------------------------------------------------------|---------------------------------------------------------------------|
| IRS | F 5'-AAGAAGTGGCGGCACAAGTC-3' R 5'-CAGCCCGCTTGTGATGTT-3' | F 5'-CTGTGTGGTTGGTTTATCATCT-3' R 5'-CATGCGTCGGTCTTTTGTACA-3' |
| PI3K | F 5'-AGCAAATGAGGCGACCAGAT-3' R 5'-ATGAGCAGGTTTATAGAGGAGACA-3' | F 5'-GGGTAGAATTGGCTCCATTGG-3' R 5'-GCTATCTCATGGCGACAAGCT-3' |
| Akt1 | F 5'-CTGAGACGCCCGGTACATG-3' R 5'-CCCCTGCCGGTCTGAATC-3' | F 5'-GCTCAACCCCATGTGTCTGA-3' R 5'-GCACCCCGCAGTGAAG-3' |
| FoxO1 | F 5'-GTGTTGCCCAACCAAGCTT-3' R 5'-CTCAGCCTGACACCAGCTAT-3' | F 5'-GAACCAGCTCAAATGCTAGTACCA-3' R 5'-GTCCCATCTCCAGGTCAT-3' |
| PEPCK | F 5'-TGGGTCGCCTCTGTCA-3' R 5'-CCACCACGTAGGGTGAATCC-3' | F 5'-TTGCGGGAAACAAGGACAAC-3' R 5'-CAGCCACTAGATTCTGGATAACTATAC-3' |
| G6Pase | F 5'-GAGTGGAGTGGCAGCATCTG-3' R 5'-GACATGAGAATCGCTTGAACCA-3' | F 5'-CAACCGCATGCAAAGG-3' R 5'-CTGGCTCACAATGGGTTTC-3' |
| GLUT2 | F 5'-TGGCAGCTGCTCAACTAATCA-3' R 5'-CCAACTGCAAAGCTGGATACAG-3' | F 5'-GGATTAAGAGGACAATCCACACA-3' R 5'-AGCCAAGTTCCGGTGATC-3' |
| GCK | F 5'-CCGACGCGAGGAGTAAT-3' R 5'-CTTGTACACGGAGCCATCCA-3' | F 5'-GCTTTTGAGACCCGTTTTGTG-3' R 5'-GCCTTCGGTCCCCAGAGT-3' |
| PFK | F 5'-GATGCCGCATACATTTTCA-3' R 5'-CTCCACGTTGGACTGCAGATC-3' | F 5'-CGACCGAATCCTGAGTAGCAA-3' R 5'-TGTCAGGCGTGCCTCTAG-3' |
| ACC | F 5'-TGGCCGGGACCCTACTCTA-3' R 5'-CTACTTTGGCATTGGTGTCTACT-3' | F 5'-TGTCCGCACTGACTGTAACCA-3' R 5'-TGCTCCGCACAGATCTTCA-3' |
| GAPDH | F 5'-CAAGGCTGTGGCAAGGT-3' R 5'-GGAAGCCATGCCAGTGA-3' | F 5'-CATGGCCTCCGTGTTCTCA-3' R 5'-GCGGCACRCAGATCCA-3' |

IRS, Insulin receptor substrate; PI3K, Phosphoinositide 3-kinases; Akt, Protein kinase B; FoxO, Forkhead box; PEPCK, Phosphoenolpyruvate carboxylase; G6Pase, Glucose 6-phosphatase; GLUT2, glucose transporter protein type 2; GCK, glucokinase; PFK, phosphofructokinase; ACC, acetyl-coA carboxylase; GAPDH, Glycerinaldehyde 3-phosphate dehydrogenase

fetal bovine serum, 1% penicillin–streptomycin, 1% sodium pyruvate, and 1% NEAA mixture. Cells were seeded at 2×10^5 cells/well in a 6-well culture plate. After incubation for 15 h, the cells were treated with 100 nM insulin or KGC05P0 (0–500 $\mu\text{g}/\text{mL}$) for 6 h and extracted to perform RT-PCR.

2.6. Experimental animals and treatments

The animal experiment was approved by the Institutional Animal Care and Use Review Committee of Kyung Hee University (KHUASP[SE]-17-026). Male C57BL/6J mice (6 weeks old, $22 \pm 1\text{g}$) and C57BLKS/J^{db/db} (db/db, 6 weeks old, $34.5 \pm 4\text{g}$) mice (60 total mice) were purchased from Saeronbio, Inc. (Uiwang, Korea). The mice were controlled in specific pathogen-free barrier facilities at $23 \pm 3^\circ\text{C}$ and 55% humidity with a 12 h light/dark cycle. The mice were acclimatized for the first week and provided a standard chow diet before experimentation, and then they were divided into six groups as follows: one C57BL/6J mice group (normal control, NC, AIN93G diet) and 5 C57BLKS/J^{db/db} mice groups (untreated control, C; positive control, PC, inulin 400 mg/kg b.w.; low, L, KGC05P0 100 mg/kg b.w.; medium, M, KGC05P0 200 mg/kg b.w.; and high, H, KGC05P0 400 mg/kg b.w.). All the experimental diets were based on the AIN93G diet. The experiment was conducted for eight weeks. The body weight, food intake, and the fasting blood glucose level were recorded weekly. Mouse urine was collected using a metabolic cage three days before the end of the experiment. After 4 h of fasting on the last day of the experiment, all mice were sacrificed and the livers were stored at -80°C until the analysis.

2.7. Oral glucose tolerance tests (OGTT)

One week before the end of the experiment, all mice were fasted for 4 h and OGTT were performed. A glucose solution (2 g/kg b.w.) was orally administered to the mice, blood samples were taken from the tail vein at 0, 30, 60, 90, and 120 min, and blood glucose levels were measured using a G. Doctor Blood Glucose Monitoring System (Allmedicus, Anyang, Korea).

2.8. ELISA assay of biochemical factors in blood, urine, and liver

A portion of the whole blood collected at the sacrifice of all experimental animals was used for hemoglobin A1c (HbA1c) measurement, using a Mouse Hemoglobin A1c Kit (Crystal Chem Inc., USA). The remaining whole blood was centrifuged (3,000 rpm at 4°C for 20 min) to collect serum samples. Glucose Assay Kits, Insulin (Mouse) ELISA Kits, Protein Carbonyl Content Assay Kit (Biovision), and a TNF- α and IL-1 β R&D Duoset ELISA kit (R&D Systems, Minneapolis, MN, USA) were used for serum or urine analysis.

The isolated liver was homogenized and lipid peroxidation was measured using the Lipid Peroxidation Colorimetric Assay Kit (Biovision). All experiments were conducted according to the specifications of the manufacturers.

2.9. Western blotting

Twenty-five-milligram samples of liver were homogenized using 0.5 mL of CellLytic™ MT Cell Lysis Reagent (Sigma-Aldrich) with Halt™ Protease and Phosphatase inhibitor Cocktail (Thermo Fisher Scientific, Rockford, IL, USA). The homogenized samples were centrifuged at 14,000 rpm at 4°C for 15 min. The protein content was measured using the Bradford assay. Protein samples (20 μg each) were loaded into 10% Mini-PROTEAN® TGX™ Precast Gels (Bio-Rad) and transferred to PVDF membranes using the Trans-Blot® Turbo™ Transfer system (Bio-Rad). The membranes were blocked with blocking buffer (5% skim milk in Tris buffered saline with 1% Tween® 20) for 1 h at room temperature. After washing, the membranes were probed overnight at 4°C with primary antibodies against β -actin, IRS-1, P-IRS-1, AKT, phospho-AKT, PI3K, and phospho-PI3K (Cell Signaling Technology, 1:1000). After washing, the membranes were incubated with horseradish peroxidase-conjugated secondary antibodies (Cell Signaling Technology, 1:2000) for 1 h at room temperature. After washing, the membranes were visualized with EzWestLumi plus (ATTO, Tokyo, Japan) using an Ez-Capture II (ATTO), and analyzed using the CS Analyzer 3.0 software (ATTO).

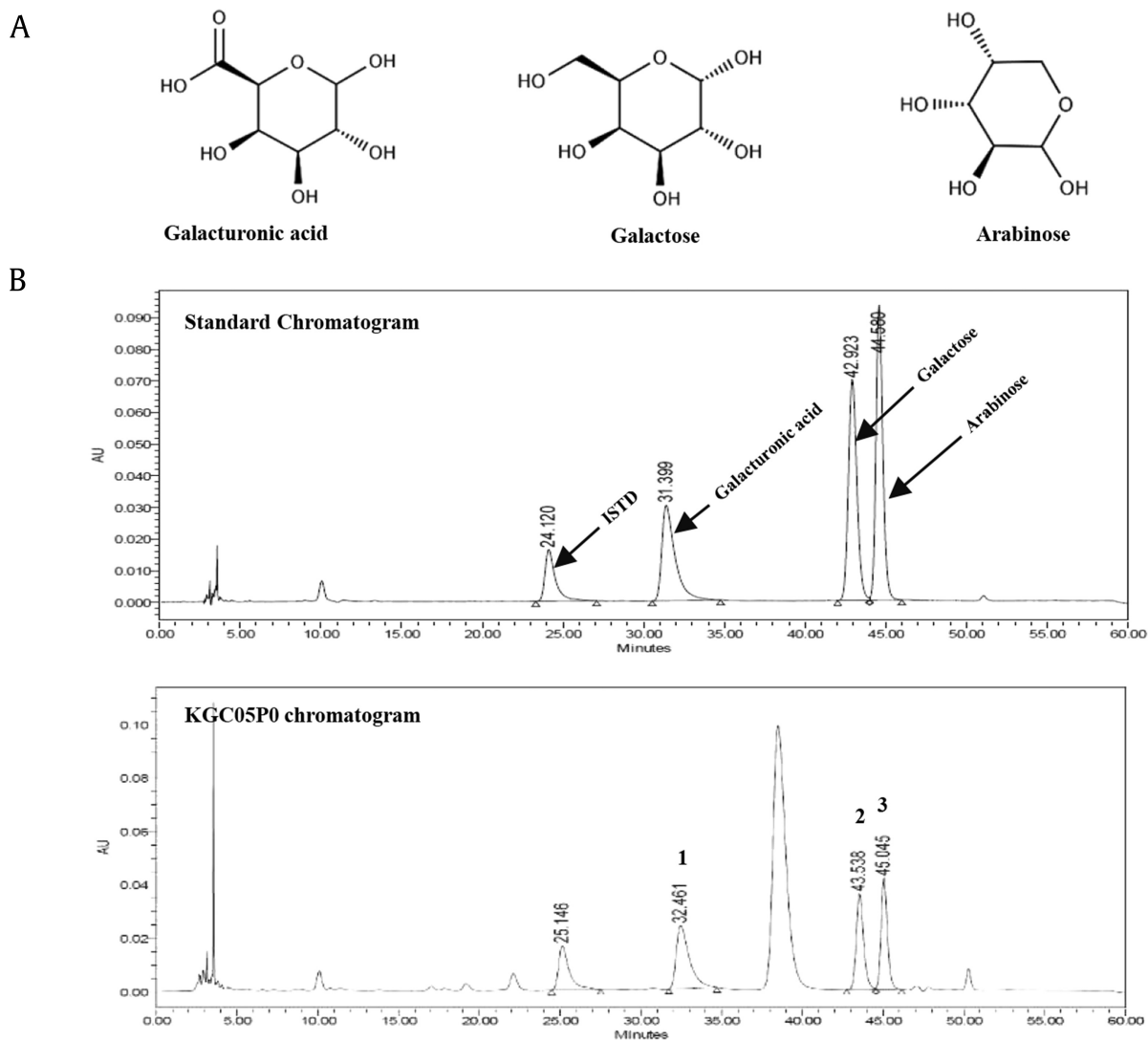


Fig. 1. HPLC chromatogram of a mixture of three standards (A) and KGC05P0 at (B) at 250 nm. Galacturonic acid (1), galactose (2), and arabinose (3) appeared with retention times of approximately 32.5 min, 43.5 min, 45.0 min, respectively.

2.10. Real-time polymerase chain reaction (PCR)

Total RNA of hepG2 cells and homogenized liver tissues were extracted using an RNeasy extraction kit (QIAGEN, Gaithersburg, MD, USA) or chloroform (Sigma-Aldrich) following the manufacturer's specifications. Purified total RNA was quantified by using a Q5000 UV-Vis spectrophotometer (Quawell, San Jose, CA, USA). cDNA was synthesized from purified total RNA by using the iScript cDNA Synthesis kit (Bio-Rad). Real-time PCR was performed by using a CFX Connect™ Real-Time System (Bio-Rad) with the iQ™ SYBR® Green Supermix (Bio-Rad), cDNA, and custom-designed primers. Then, the cDNA was amplified with 40 cycles of denaturation (95°C for 15 s), annealing (56°C for 30 s), and extension (72°C for 30 s). Data analysis was conducted by using the CFX Manager Software 3.1 (Bio-Rad). The gene sequences are shown in Table 1.

2.11. Statistical analysis

All experimental results are expressed as mean \pm standard deviation (SD). The significance of differences was determined with a

one-way analysis of variance (ANOVA) and Duncan's multiple-range test using the SPSS PASW Statistic 22.0 (SPSS, Inc., Chicago, IL, USA). Values of $P < 0.05$ were considered statistically significant.

3. Results

3.1. HPLC analysis of KGC05P0

The HPLC analysis of the KGC05P0 revealed three peaks matching those of the commercial standards galacturonic acid, galactose, and arabinose, with retention times of approximately 32.5 min, 43.5 min, 45.0 min, respectively (Fig. 1). The KGC05P0 contained 23.62 mg/g galacturonic acid, 15.93 mg/g galactose, and 14.08 mg/g arabinose.

3.2. Inhibitory effects of KGC05P0 on α -glucosidase and α -amylase *in vitro*

KGC05P0 inhibited α -glucosidase activity in a dose-dependent manner by 20.1, 23.9, 25.3, 25.3, 29.5, and 41.5% compared with

the control group at 100, 300, 500, 700, 1000, and 2000 $\mu\text{g/mL}$ ($P < 0.05$) (Fig. 2A). KGC05P0 inhibited α -amylase activity in a dose-dependent manner by 46.5, 57.05, 64.15, 69.2, 72.7, and 73.1% compared with the control group at 100, 300, 500, 700, 1000, and 2000 $\mu\text{g/mL}$ ($P < 0.05$) (Fig. 2B). Furthermore, the KGC05P0 was more effective than inulin at the same concentration in terms of α -glucosidase and α -amylase inhibition. In addition, the inhibitory activity of both enzymes did not exceed the inhibitory effect of acarbose, a commercially obtained inhibitor.

3.3. Effects of KGC05P0 on glucose uptake and transport rate in Caco-2 cells

Prior to the experiment, the viability of Caco-2 cells treated with KGC05P0 was tested; KGC05P0 was not cytotoxic up to a concentration of 500 $\mu\text{g/mL}$ (data not shown). KGC05P0 caused a statistically significant reduction of glucose uptake in a dose-dependent manner: 29.2, 40.0, 48.8, and 55.1% compared to the control group at 200, 300, 400, and 500 $\mu\text{g/mL}$, respectively, in Caco-2 cells ($P < 0.05$) (Fig. 3A). In addition, the glucose permeability rate of Caco-2 cells was significantly decreased: 36.7, 37.4, and 40.0% compared to the control group at 300, 400, and 500 $\mu\text{g/mL}$, respectively ($P < 0.05$) (Fig. 3B).

3.4. Down-regulation effects of KGC05P0 on gluconeogenesis pathway-related mRNA expression in HepG2 cell

Prior to the experiment, cell viability of KGC05P0 on HepG2 cells was tested and was not cytotoxic up to a concentration of 500 $\mu\text{g/mL}$ (data not shown). The mRNA expressions of IRS1 of KGC05P0 groups were increased in a dose-dependent manner compared to the control group, but was significantly higher in 300 and 500 groups. The mRNA expressions of PI3K, AKT, and forkhead box 1 (FoxO1) of KGC05P0 groups were significantly increased in a dose-dependent manner compared to the control group. The mRNA expressions of PEPCK and G6Pase of KGC05P0 groups were significantly decreased in a dose-dependent manner compared to the control group. The mRNA expressions of glucose transporter protein type 2 (GLUT-2) of KGC05P0 groups were significantly increased in a dose-dependent manner compared to the control group. The mRNA expressions of GCK, PFK, and ACC of KGC05P0 groups were significantly increased in a dose-dependent manner compared to the control group. In particular, KGC05P0 showed a

greater effect at the same dose compared to the inulin groups ($P < 0.05$) (Table 2).

3.5. Effects of KGC05P0 on body weight, food intake, food efficiency rate, water intake, and urine excretion of diabetic mice

This study showed a significant increase in weight gain in the C57BLKS/J^{db/db} groups compared to the normal control (5.43 ± 1.03 g) group. In particular, the weight gains of the KGC05P0 100, 200, and 400 groups (11.69 ± 4.50 g, 9.99 ± 4.20 g, and 8.53 ± 2.22 g) were significantly decreased compared to the control (15.43 ± 4.63 g) group. There were also no significant differences in food efficiency rate among the C57BLKS/J^{db/db} groups. Also, the amounts of water intake and urine excretion were significantly increased in the C57BLKS/J^{db/db} groups compared to the normal control and were significantly decreased in a dose-dependent manner in the groups fed KGC05P0-containing diets compared to the normal control group ($P < 0.05$) (Table 3).

3.6. Effects of KGC05P0 on glucose level and glucose tolerance in diabetic mice over eight weeks

The blood glucose levels of the C57BLKS/J^{db/db} groups gradually increased until eight weeks compared with the normal control group. Also, the blood glucose levels measured at eight weeks decreased in a dose-dependent manner in the groups fed with the KGC05P0-containing diet compared to the control group (559.00 ± 35.94 mg/dL) ($P < 0.05$) (Fig. 4A).

As shown by OGTT, the blood glucose level of the control group was highest at 30 min after oral glucose administration (832.33 ± 18.93 mg/dL) compared to the fasting state, and the blood glucose level gradually decreased over the following 90 min, but the control group still had the highest value (662.33 ± 5.51 mg/dL) at 120 min post challenge compared with the other groups. In the groups fed with KGC05P0-containing diets, the blood glucose levels measured at 30 min after oral glucose administration increased significantly compared to the normal control group, but were lower than that of the control group. In addition, the blood glucose levels gradually decreased in a dose-dependent manner through 120 min compared with the control group ($P < 0.05$) (Fig. 4B).

The total area under the curve (AUC) was calculated by the trapezoid rule during the OGTT. The AUC in the groups fed with

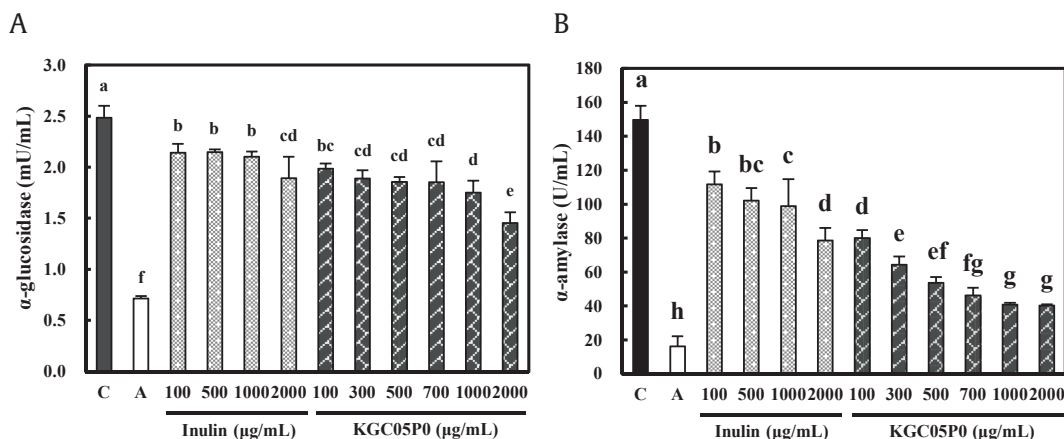


Fig. 2. Inhibitory effects of KGC05P0 on α -glucosidase and α -amylase. (A) α -Glucosidase. (B) α -Amylase. Values are presented as mean \pm SD ($n = 3$), and different alphabets indicate significance at $P < 0.05$. C, control; A, acarbose (1000 $\mu\text{g/mL}$).

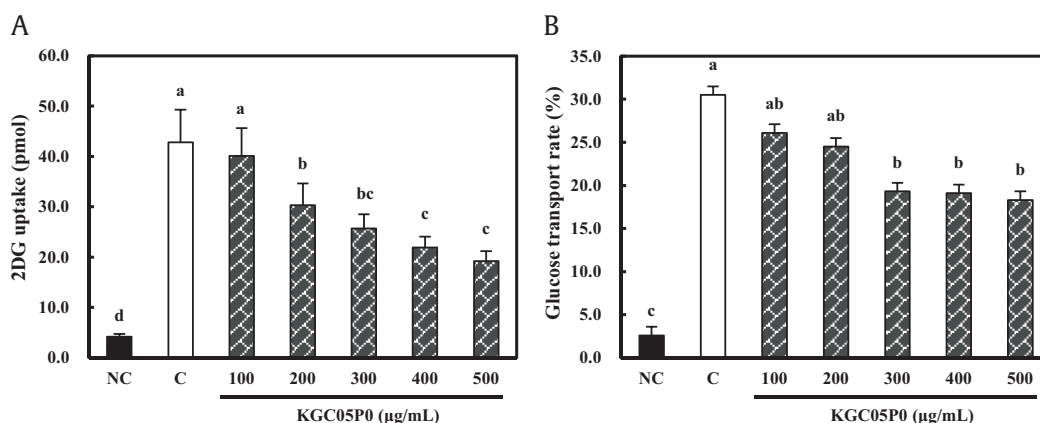


Fig. 3. Effects of KGC05P0 on glucose transport by Caco-2 cells under sodium-dependent conditions. (A) 2DG uptake. (B) Transport rate. Values are presented as mean \pm SD ($n = 3$), and different alphabets indicate significance at $P < 0.05$. NC, normal control; C, control.

KGC05P0-containing diets significantly decreased in a dose-dependent manner compared to the control group ($P < 0.05$) (Fig. 4C).

3.7. Effects of KGC05P0 on blood biochemical factors in diabetic mice

The effects of KGC05P0 on blood biochemical factors in mice are shown in Table 3. The level of insulin in the control group was significantly decreased compared to the normal control group, and the levels in the groups fed KGC05P0-containing diets were significantly increased in a dose-dependent manner compared to the control group (all $P < 0.05$). The homeostasis model assessment of insulin resistance (HOMA-IR) was significantly increased in the C57BLKS/J^{db/db} groups compared to the normal control group ($P < 0.05$), and the HOMA-IR of the groups fed with KGC05P0-containing diets were decreased compared to the control group. However, there were no significant differences among the groups fed KGC05P0-containing diets.

The levels of HbA1c and carbonyl in the control group ($11.32 \pm 1.49\%$ and 12 ± 0.70 nmol/mg, respectively) were significantly increased compared to the normal control group ($5.91 \pm 0.91\%$ and 6.09 ± 1.17 nmol/mg, respectively), and the groups fed with KGC05P0-containing diets were significantly decreased in a dose-dependent manner compared to the control group (all $P < 0.05$).

The levels of proinflammatory cytokines (TNF- α and IL-1 β) in the control group (441.75 ± 22.39 pg/mL and 14.75 ± 1.07 pg/mL, respectively) were significantly increased compared to the normal control group (113.08 ± 22.45 pg/mL and 7.32 ± 0.65 pg/mL, respectively), and those of the groups fed with KGC05P0-containing diets were significantly decreased in a dose-dependent manner compared to the control group (all $P < 0.05$).

3.8. Effects of KGC05P0 on urine glucose levels in diabetic mice

The level of urine glucose in the control group (9.88 ± 0.94 mg/dL) was significantly increased compared to the normal control group (0.34 ± 0.18 mg/dL), and those of the groups fed with KGC05P0-containing diets were significantly decreased compared to the control group (all $P < 0.05$). However, there were no significant differences among the groups fed with KGC05P0-containing diets (Table 3).

3.9. Effects of KGC05P0 on hepatic lipid peroxidation (LPO) in diabetic mice

The level of hepatic LPO in the control group (1.37 ± 0.12 nmol/mg) was significantly increased compared to the normal control group (0.53 ± 0.10 nmol/mg), and those of the groups fed with KGC05P0-containing diets were significantly decreased in a dose-dependent manner compared to the control group ($P < 0.05$). In

Table 2
Effects of KGC05P0 on basal and insulin action on gluconeogenesis pathway-related mRNA levels in HepG2 cells

| Gene description | NC | C | PC | KGC05P0 | | |
|------------------|------------------------------|-------------------------------|-------------------------------|-------------------------------|-------------------------------|------------------------------|
| | | | | 100 | 300 | 500 |
| IRS1 | 1.00 \pm 0.08 ^c | 1.42 \pm 0.27 ^b | 1.83 \pm 0.04 ^a | 1.59 \pm 0.11 ^b | 1.87 \pm 0.11 ^a | 2.05 \pm 0.06 ^a |
| PI3K | 1.00 \pm 0.09 ^c | 1.42 \pm 0.10 ^d | 1.86 \pm 0.08 ^{ab} | 1.59 \pm 0.07 ^c | 1.75 \pm 0.07 ^{bc} | 1.96 \pm 0.12 ^a |
| AKT | 1.00 \pm 0.20 ^c | 1.06 \pm 0.10 ^c | 1.48 \pm 0.07 ^{ab} | 1.33 \pm 0.06 ^{bc} | 1.45 \pm 0.01 ^{ab} | 1.60 \pm 0.11 ^a |
| FoxO1 | 1.00 \pm 0.13 ^d | 1.18 \pm 0.09 ^c | 1.37 \pm 0.05 ^b | 1.39 \pm 0.04 ^b | 1.60 \pm 0.03 ^a | 1.68 \pm 0.07 ^a |
| PEPCK | 1.00 \pm 0.05 ^a | 0.90 \pm 0.06 ^a | 0.54 \pm 0.05 ^c | 0.73 \pm 0.06 ^b | 0.51 \pm 0.08 ^c | 0.40 \pm 0.05 ^d |
| G6Pase | 1.00 \pm 0.26 ^a | 0.83 \pm 0.13 ^{ab} | 0.49 \pm 0.05 ^{cd} | 0.64 \pm 0.05 ^{bc} | 0.35 \pm 0.04 ^{de} | 0.23 \pm 0.04 ^e |
| GLUT2 | 1.00 \pm 0.13 ^a | 0.65 \pm 0.05 ^c | 0.75 \pm 0.04 ^{hc} | 0.75 \pm 0.03 ^{bc} | 0.82 \pm 0.01 ^b | 0.95 \pm 0.05 ^a |
| GCK | 1.00 \pm 0.12 ^d | 2.10 \pm 0.16 ^c | 2.36 \pm 0.12 ^{bc} | 2.37 \pm 0.11 ^{bc} | 2.68 \pm 0.16 ^b | 3.24 \pm 0.36 ^a |
| PFK | 1.00 \pm 0.20 ^b | 1.28 \pm 0.07 ^b | 1.78 \pm 0.44 ^a | 1.84 \pm 0.04 ^a | 2.19 \pm 0.20 ^a | 2.20 \pm 0.17 ^a |
| ACC | 1.00 \pm 0.29 ^d | 1.23 \pm 0.01 ^c | 1.46 \pm 0.07 ^{bc} | 1.53 \pm 0.02 ^b | 1.64 \pm 0.02 ^{ab} | 1.84 \pm 0.12 ^a |

All groups were stimulated with 100 nM insulin for 6 h except normal control group. Insulin receptor substrate (IRS1), Phosphoinositide 3-kinases (PI3K), Protein kinase B (AKT), Forkhead box 1 (FoxO1), Phosphoenolpyruvate carboxykinase (PEPCK), Glucose 6-phosphatase (G6Pase), glucose transporter protein type 2 (GLUT2), Glucokinase (GCK), Phosphofructokinase (PFK), and Acetyl-CoA carboxylase (ACC) mRNA expressions were assessed by RT-PCR. Values are presented as mean \pm SD ($n = 3$), and different alphabets indicate significance at $P < 0.05$. NC, normal control; C, control; PC, positive control (inulin 500 μ g/mL); KGC05P0 (100, 300, 500 μ g/mL)

Table 3Effects of KGC05P0 on weight gain, food intake and FER and parameters in blood and urine of C57BLKS/J^{db/db} mice

| Variables | NC | C57BLKS/J ^{db/db} | | | | |
|------------------------------|-----------------------------|-----------------------------|-----------------------------|----------------------------|------------------------------|-----------------------------|
| | | C | PC | L | M | H |
| Variables | | | | | | |
| Weight gain (g) ¹ | 5.43 ± 1.03 ^c | 15.43 ± 4.63 ^a | 12.31 ± 4.51 ^{ab} | 11.69 ± 4.50 ^{ab} | 9.99 ± 4.20 ^{bc} | 8.53 ± 2.22 ^{bc} |
| Food intake (g/day/mouse) | 2.32 ± 0.13 ^f | 4.25 ± 0.40 ^a | 3.90 ± 0.33 ^e | 3.96 ± 0.35 ^d | 4.17 ± 0.58 ^b | 4.08 ± 0.27 ^c |
| Water intake (mL/day) | 3.00 ± 1.00 ^d | 18.00 ± 2.65 ^a | 6.33 ± 2.89 ^c | 15.33 ± 0.58 ^a | 12.00 ± 1.73 ^b | 9.33 ± 0.58 ^{bc} |
| Urine excretion (mL/day) | 0.50 ± 0.23 ^e | 15.33 ± 1.53 ^a | 5.78 ± 2.20 ^d | 11.67 ± 0.58 ^b | 9.00 ± 1.00 ^c | 7.33 ± 0.58 ^{cd} |
| FER ² | 4.34 ± 0.82 ^{bc} | 6.93 ± 2.82 ^a | 6.30 ± 0.31 ^{ab} | 5.50 ± 2.12 ^{abc} | 4.39 ± 1.85 ^{bc} | 3.89 ± 1.01 ^c |
| Blood | | | | | | |
| Glucose (mg/dL) | 172.67 ± 24.35 ^d | 559.00 ± 35.94 ^a | 367.60 ± 32.28 ^c | 433.25 ± 5.38 ^b | 395.20 ± 41.81 ^{bc} | 367.33 ± 51.18 ^c |
| Insulin (μU/mL) | 7.36 ± 0.48 ^a | 4.06 ± 0.35 ^d | 6.41 ± 0.66 ^{bc} | 4.45 ± 0.21 ^d | 6.08 ± 0.44 ^c | 6.62 ± 0.51 ^b |
| HOMA-IR ³ | 3.14 ± 0.49 ^c | 5.66 ± 0.51 ^a | 5.64 ± 0.35 ^a | 4.76 ± 0.25 ^b | 5.53 ± 0.35 ^a | 5.37 ± 0.98 ^{ab} |
| HbA1c (%) | 5.91 ± 0.91 ^d | 11.32 ± 1.49 ^a | 6.88 ± 0.38 ^{cd} | 9.93 ± 0.71 ^b | 7.50 ± 0.42 ^c | 6.61 ± 0.71 ^{cd} |
| Carbonyl (nmol/mg prot.) | 6.09 ± 1.17 ^d | 12.16 ± 0.70 ^a | 7.56 ± 0.66 ^c | 11.17 ± 1.02 ^a | 9.22 ± 0.84 ^b | 7.14 ± 0.52 ^{cd} |
| TNF-α (pg/mL) | 113.08 ± 22.45 ^e | 441.75 ± 22.39 ^a | 288.25 ± 7.20 ^c | 325.58 ± 8.76 ^b | 302.25 ± 14.47 ^c | 249.75 ± 15.49 ^d |
| IL-1β (pg/mL) | 7.32 ± 0.65 ^e | 14.75 ± 1.07 ^a | 12.21 ± 0.65 ^c | 13.17 ± 0.97 ^b | 11.71 ± 0.35 ^c | 10.65 ± 0.43 ^d |
| Urine | | | | | | |
| Glucose (mg/dL) | 0.34 ± 0.18 ^d | 9.88 ± 0.94 ^a | 6.68 ± 0.15 ^c | 8.63 ± 0.37 ^b | 7.88 ± 0.99 ^b | 7.90 ± 0.74 ^b |

Values are presented as mean ± standard deviation (n = 8), and different superscript letters indicate significance at P < 0.05

NC, normal control; C, control; PC, positive control (inulin 400 mg/kg b.w.); L (KGC05P0 100 mg/kg b.w.); M (KGC05P0 200 mg/kg b.w.); H (KGC05P0 400 mg/kg b.w.); HbA1c, glycated hemoglobin; TNF-α, tumor necrosis factor alpha; IL-1β, interleukin-1 beta

¹ Weight gain (g/12 weeks) = final body weight (g) – initial body weight (g).² FER (food efficiency rate) = weight gain (g)/total food consumption (g) × 100.³ HOMA-IR (homeostasis model assessment of insulin resistance) = fasting insulin (μU/mL) × fasting glucose (mg/dL)/405.

particular, the level of LPO in the H group (0.58 ± 0.07 nmol/mg) was the lowest among the groups fed with KGC05P0-containing diets, and it was not significantly different from the positive control (0.48 ± 0.07 nmol/mg) and normal control groups (Fig. 4D).

3.10. Down-regulation effects of KGC05P0 on gluconeogenesis pathway-related protein and mRNA expression in the livers of diabetic mice

The expression levels of IRS-1 and p-IRS-1 were significantly inhibited in the control group compared to the normal control group, and those in the groups fed with the KGC05P0-containing diets were increased in a dose-dependent manner compared to the control group at the protein and mRNA levels (all P < 0.05) (Fig. 5A and B). The phospho-PI3K/PI3K ratio and phospho-AKT/AKT ratio were significantly decreased in the control group compared to the normal group, and those in the groups fed with KGC05P0-containing diets were significantly increased in a dose-dependent manner compared to the control group, at the protein and mRNA levels (mRNA data not shown) (P < 0.05) (Fig. 5A, C, and D). The expression of FoxO1 was significantly decreased in the control group compared to the normal control group, and those of the groups fed with KGC05P0-containing diets were increased in a dose-dependent manner compared to the control group, at the mRNA level (P < 0.05) (Fig. 5E). The expression levels of G6Pase and PEPCK were significantly increased in the control group compared to the normal control group, and those in the groups fed with KGC05P0-containing diets were decreased in a dose-dependent manner compared to the control group, at the mRNA level (P < 0.05) (Fig. 5F and G). The expression of GLUT2 was significantly decreased in the control group compared to the normal control group, and those of the groups fed with KGC05P0-containing diets were increased in a dose-dependent manner compared to the control group, at the mRNA level (P < 0.05) (Fig. 5H). The expression levels of GSK, PFK, and ACC were significantly increased in the control group compared to the normal control group, and those in the groups fed with KGC05P0-containing diets were increased in a dose-dependent manner compared to the control group, at the mRNA level (P < 0.05) (Fig. 5I, J, and K).

4. Discussion

A healthy diet is an essential factor in lowering the risk of developing T2DM. T2DM, a chronic metabolic disease, is characterized by insulin resistance and insufficient insulin secretion [18]. Some medications for T2DM have several limitations, such as adverse effects and high secondary failure rates [19]. Therefore, interest in food materials without adverse effects is increasing, and the market for health functional foods is increasing year by year.

RG, a popular functional food among Asian people, and saponin, its active ingredient, have been reported to have anti-diabetic effects such as controlling blood glucose and insulin resistance [20–22]. However, the absolute content of saponin in the thick root (main root), which is recognized as an important medicinal site of ginseng, is significantly less than that of the fine root. This suggests that the non-saponin components include an active ingredient. The non-saponin components include polysaccharides, maltulosyl arginine, protein fraction, polypeptides, polyacetylene compounds, phenol compounds, alkaloids, and lignans [23]. In particular, many studies have shown that polysaccharides of natural products have anti-diabetic effects [24]. Among them, galacturonic acid, galactose, and arabinose are present in various plants [25–27]. Our HPLC analysis showed that KGC05P0 contained galacturonic acid, galactose, and arabinose. In addition, there are several studies on the effects of the non-saponin fraction on platelet aggregation, learning deficits, immunomodulation, and multi-drug resistance [28–31], but little is known about its anti-diabetic effect.

In this study, we focused on whether KGC05P0, a non-saponin fraction of Korean Red Ginseng, has anti-diabetic activity *in vitro* and *in vivo*. KGC05P0 showed stronger inhibitory activity against both α-glucosidase and α-amylase compared with inulin, a functional food, but its activity was not stronger than that of acarbose (1000 μg/mL), a carbohydrate digestive enzyme inhibitor [32]. Acarbose (IC50 = 1000 μg/mL) is frequently used for the treatment of T2DM and has been tested at concentrations up to 1000 μg/mL in several studies [33,34]. It has been reported that polysaccharides obtained from *Camellia sinensis* leaves and flowers have inhibitory activity against α-glucosidase and α-amylase and thus may prevent diabetes [35]. In addition, phenolic compounds, alkaloids, and polypeptides are known to act as inhibitors of α-glucosidase and α-

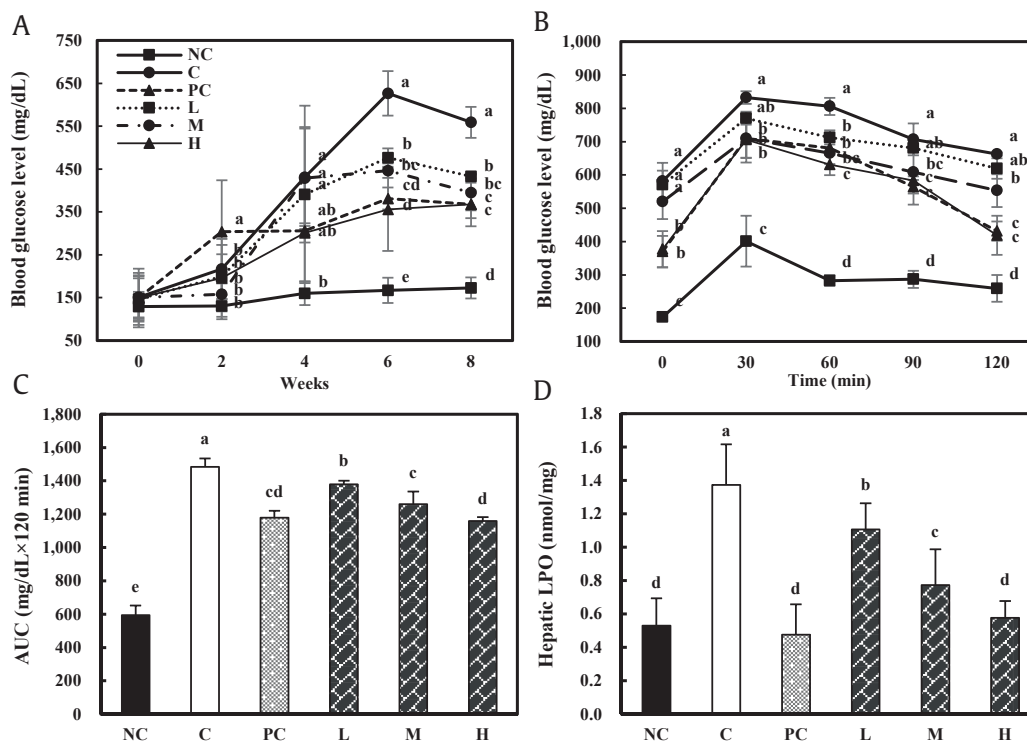


Fig. 4. Effects of KGC05P0 on glucose levels and hepatic profile in C57BL/6J and C57BLKS/J^{db/db} mice. (A) Weekly glucose level. (B) Oral glucose tolerance tests (OGTT). (C) Total area under the curve (AUC). (D) Hepatic lipid peroxidation (LPO). Values are presented as mean \pm SD ($n = 10$), and different alphabets indicate significance at $P < 0.05$. NC, normal control; C, control; PC, positive control (Inulin, 400 mg/kg b.w.); L, low (KGC05P0 100 mg/kg b.w.); M, medium (KGC05P0 200 mg/kg b.w.); H, high (KGC05P0 400 mg/kg b.w.).

amylase [36–38]. The inhibition of α -glucosidase and α -amylase activities in the digestive tract was reported to inhibit diabetes by reducing the absorption of glucose degraded from starch [32].

In addition, glucose uptake in the digestive tract controls blood glucose levels, and repeated high postprandial glucose levels are associated with severe metabolic disease and an increased risk of T2DM [39]. In this study, KGC05P0 significantly reduced the glucose uptake and glucose transport rate compared to the control group in Caco-2 cells. Caco-2 cells have been widely used in dietary polyphenol transport and metabolism studies, and are suitable for glucose uptake and transport studies because of their abundant expression of glucose transport proteins and sodium-dependent glucose transporters [39].

Glucose transport is the most fundamental process in energy metabolism, and the permeation of glucose into small intestinal cells plays a key role in metabolic regulation. Recently, it has been reported that polyphenols and phenolic acids, which are bioactive compounds, can affect the uptake, transport, and blood level of glucose [40,41]. In addition, more studies are investigating the interaction of transporters with enzymes and polyphenols of importance to glucose uptake and metabolism [42,43]. Therefore, it is worthwhile to confirm the uptake and transport level of glucose after treatment with KGC05P0, a non-saponin fraction of Korean Red Ginseng, and further experiments should be conducted to confirm the expression of glucose transport proteins and sodium-dependent glucose transporters.

OGTT is one of the most important criteria for assessing hypoglycemic effects [44]. KGC05P0 is expected to increase glucose utilization because it significantly lowers blood glucose levels and significantly inhibits its increase during OGTT in diabetic mice. The serum insulin level in the KGC05P0-treated diabetic mice was significantly controlled compared to the control group. In addition,

KGC05P0 significantly decreased HbA1c, carbonyl contents, TNF- α , and IL-1 β levels compared to the control group among diabetic mice. HbA1c is a crucial biomarker that shows the severity of hyperglycemia. HbA1c levels are a useful measure of overall blood glucose control because they reflect accumulated glycation over the lifetime of red blood cells [45]. Hyperglycemia leads to the production of glycosylated hemoglobin through non-enzymatic glycation and oxidation of proteins such as hemoglobin and insulin. When additional denaturation occurs thereafter, irreversible products of final glycation are formed, leading to insulin resistance and diabetic complications. The production of glycated hemoglobin and the final glycation end product is also highly correlated with production of inflammatory factors. The proinflammatory cytokines TNF- α and IL-1 β induce structural changes in insulin and promote the formation of glycated hemoglobin, and also cause the production of the advanced glycation end products [46]. In addition, increased urinary glucose, a typical symptom of T2DM, indicates the occurrence of postprandial hyperglycemia and hepatic glucose output, as they lead to an increase in fasting glucose and urinary glucose excretion [47]. Urinalysis studies have demonstrated that KGC05P0 significantly reduces urinary glucose excretion compared to the control group.

The liver plays an important role in maintaining glucose levels by lowering the glucose level in circulation in the post-meal state and supplying glucose through gluconeogenesis and glycogenolysis in the fasting state [48]. However, abnormal glucose metabolism in the liver is the main characteristic of diabetes; abnormal activation of the glucose production pathway leads to elevated glucose levels in the blood and insulin resistance in the liver [48,49]. In our study, KGC05P0 significantly inhibited the PI3K/AKT pathway and increased the expression of G6Pase and PEPCK in the livers of diabetic mice. The binding of insulin to the IR leads to an increase in

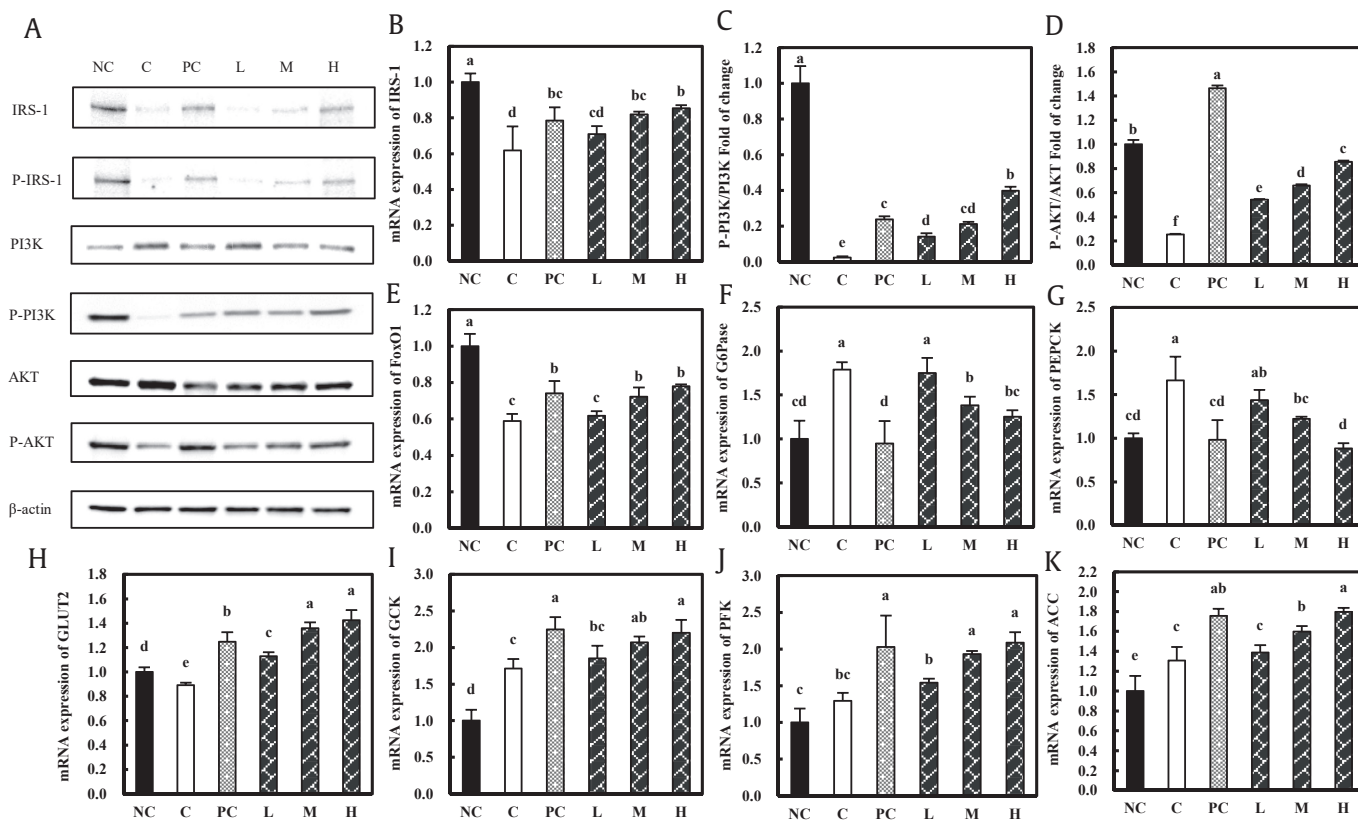


Fig. 5. Effects of KGC05P0 on protein and mRNA expression in liver from C57BL/6J and C57BLKS/J^{db/db} mice. (A) Protein expressions, (B) mRNA expression of IRS-1, (C) the ratio of phosphorylated/total PI3K protein expression, (D) the ratio of phosphorylated/total AKT protein expression, (E) FoxO1 mRNA expression, (F) G6Pase mRNA expression, (G) PEPCK mRNA expression, (H) GLUT2 mRNA expression, (I) glucokinase mRNA expression, (J) phosphofructokinase mRNA expression, and (K) acetyl-CoA carboxylase mRNA expressions. Values are presented as mean \pm SD, and different alphabets indicate significance at $P < 0.05$. NC, normal control; C, control; PC, positive control (inulin, 400 mg/kg b.w.); L, low (KGC05P0 100 mg/kg b.w.); M, medium (KGC05P0 200 mg/kg b.w.); H, high (KGC05P0 400 mg/kg b.w.).

IRS-1/2 expression and stimulates the PI3K/AKT pathway, which are needed for the suppression of gluconeogenic genes such as G6Pase and PEPCK in the liver [4,50]. PI3K is a secondary messenger that plays a crucial role in cellular signaling. PI3K comprises a regulatory subunit p85 and a catalytic subunit p110, and quantitative imbalance of the PI3K subunits can induce insulin resistance. AKT is an important downstream node of PI3K, and activation of AKT inhibits the expression of G6Pase and PEPCK through FoxO1 phosphorylation [51,52]. Padiya and Liu confirmed that the phosphorylated forms of PI3K and AKT in the diabetic model decreased compared to the total expression level and increased again by Galic or Irisin treatment [53,54]. Several studies have shown that (–)-epicatechin, phenolic extract, and naringenin stimulate the AKT pathway in HepG2 cells [55–57], and polyphenols of green tea also increased the expression of the PI3K/AKT levels in the livers in rat models of insulin resistance [58]. G6Pase and PEPCK are important factors controlling hepatic glucose output and AG-dieckol is known to decrease their activities in db/db mice [59–61].

GLUT-2 is primarily located in the liver cell membrane. There are many studies that showed that GLUT-2 is needed for glucose-stimulated insulin secretion, and glycemic controlling in response to dietary intake [62–64]. In our study, KGC05P0 significantly increased GLUT-2 mRNA expression *in vitro* and *in vivo* and the result shows that KGC05P0 may facilitate the transport of blood glucose into the liver. In glycolysis pathway, it is shown that the GCK, PFK enzyme activities and their mRNA levels are decreased in diabetic liver [65]. ACC is an enzyme involved in converting glucose

into fat after pyruvate generates energy through the TCA cycle [66,67]. Interestingly, in this study we confirm that the mRNA levels of GCK, PFK, and ACC were significantly increased in the KGC05P0 groups compared to the control group. Taken together, the increased mRNA levels of these observed in this study implicate that KGC05P0 enhances glycolysis to regulate glucose level and not only converts glucose into fat, but also improve insulin resistance in the diabetic liver.

5. Conclusion

In conclusion, we observed evidence that KGC05P0, isolated from the non-saponin fraction of Korean Red Ginseng, can inhibit the digestion and absorption of glucose through inhibition of α -glucosidase, α -amylase, glucose uptake, and glucose transport *in vitro*. In addition, our study shows that KGC05P0 has anti-diabetic activities in C57BLKS/J^{db/db} mice. KGC05P0 regulated hyperglycemia and glucose tolerance and the levels of insulin, HbA1c, carbonyl contents, and proinflammatory cytokines in blood. It also decreased glucose excretion in the urine in diabetic mice. In addition, we found that KGC05P0 regulates glucose level by down regulating the PI3K/AKT pathway and enhancing glycolysis. Although further experiments are required to define the precise role of KGC05P0 in relation to the glucose transport pathway, KGC05P0 is known to contain abundant polysaccharides, phenol compounds, and other active substances, which can be useful as hyperglycemic foods.

Conflicts of interest

The authors declare that they have no conflicts of interest.

Acknowledgments

This work was supported by research funding from the Korea Ginseng Corporation.

References

- Oh MJ, Kim HJ, Park EY, Ha NH, Song MG, Choi SH, Chun BG, Kim DH. The effect of Korean Red Ginseng extract on rosiglitazone-induced improvement of glucose regulation in diet-induced obese mice. *J Ginseng Res* 2017;52–9.
- Ahn J, Um MY, Lee H, Jung CH, Heo SH, Ha TY. Eleutheroside E, an active component of *Eleutherococcus senticosus*, ameliorates insulin resistance in type 2 diabetic db/db mice. *Evid Based Complement Alternat Med* 2013; 934183.
- Kwon HO, Lee MH, Kim YJ, Kim E, Kim OK. Beneficial effects of *Acanthopanax senticosus* extract in type II diabetes animal model via down-regulation of advanced glycosylated hemoglobin and glycosylation end products. *J Korean Soc Food Sci* 2016;45(7):929–37.
- Cordero-Herrera I, Martin MA, Bravo L, Goya L, Ramos S. Cocoa flavonoids improve insulin signalling and modulate glucose production via AKT and AMPK in HepG2 cells. *Mol Nutr Food Res* 2013;57:974–85.
- Elieen LW, Han C, Birnbaum MJ. Role of Akt protein kinase B in metabolism. *Trends in Endocrinol Metab* 2002;13(10):444–51.
- Shepherd PR, Withers DJ, Siddle L. Phosphoinositide 3-kinase: the key switch mechanism in insulin signalling. *Biochem J* 1998;333(3):471–90.
- Nakae J, Kitamura T, Silver DL, Accili D. The forkhead transcription factor Foxo1 (Fkhr) confers insulin sensitivity onto glucose-6-phosphatase expression. *J Clin Invest* 2001;108:1359–67.
- Puigserver P, Rhee J, Donovan J, Walkey CJ, Toon JC, Oriente F, Kitamura Y, Altomonte J, Dong H, Accili D, et al. Insulin-regulated hepatic gluconeogenesis through FOXO1-PGC-1 α interaction. *Nature* 2003;423:550–5.
- Alpers CE, Hudkins KL. Mouse models of diabetic nephropathy. *Curr Opin Nephrol Hypertens* 2011;20:278–84.
- Sharma K, McCue P, Dunn SR. Diabetic kidney disease in the db/db mouse. *An J Physiol Renal Physiol* 2003;284:F1138–44.
- Yang HN, Son WS, Park HR, Lee SE, Park YS. Effect of Korean red ginseng treatment on the gene expression profile of diabetic rat retina. *J Ginseng Res* 2016;40:1–8.
- Yun TK, Zheng S, Choi SY, Cai SR, Lee YS, Liu XY, Cho KJ, Park KY. Non-organ-specific preventive effect of long-term administration of Korean red ginseng extract on incidence of human cancers. *J Med Food* 2010;13(3):489–94.
- Kim JH, Yi YS, Kim MY, Cho JY. Role of ginsenosides, the main active components of *Panax ginseng*, in inflammatory responses and diseases. *J Ginseng Res* 2017;41:435–43.
- Patel SB, Santani D, Patel V, Shah M. Anti-diabetic effects of ethanol extract of AMPK compensatory effects for ER stress-mediated beta-cell dysfunction during the progression of type-2 diabetes. *Cell Signal* 2013;25:2348–61.
- Kim HY, Kim K. Protective effect of ginseng on cytokine-induced apoptosis in pancreatic beta-cells. *J Agric Food Chem* 2007;55:2816–23.
- Lim KH, Cho JY, Kim B, Bae BS, Kim JH. Red ginseng (*Panax ginseng*) decreases isoproterenol-induced cardiac injury via antioxidant properties in porcine. *J Med Food* 2014;17:111–8.
- Kuate D, Kengne AP, Biapa CP, Azantus BG, Abdul Manan Bin Wan Muda W. Tetrapleura tetraptera spice attenuates high-carbohydrate, high-fat diet induced obese and type 2 diabetic rats with metabolic syndrome features. *Lipids Health Dis* 2015;14:50.
- Nishina PM, Naggert JK, Verstuyft J, Paigen B. Atherosclerosis in genetically obese mice: the mutants obese, diabetes, fat, tubby, and lethal yellow. *Metabolism* 1994;5:554–8.
- Lee SH, Min KH, Han JS, Lee DH, Park DB, Jung WK, Park PJ, Jeon BT, Kim SK, Jeon YJ. Effects of brown alga, *Ecklonia cava* on glucose and lipid metabolism in C57BL/KsJ-db/db mice, a model of type 2 diabetes mellitus. *Food Chem Toxicol* 2012;50:575–82.
- Vuksan V, Sung MK, Sievenpiper JL, Stravro PM, Jenkins AL, Buono MD, Lee KS, Leiter LA, Nam KY, Armonson JT, et al. Korean red ginseng (*Panax ginseng*) improves glucose and insulin regulation in well-controlled, type 2 diabetes: results of a randomized, double-blind, placebo-controlled study of efficacy and safety. *Nutr Metabol Cardiovasc Dis* 2008;18:46–56.
- Bang HJ, Kwak JH, Ahn HY, Shin DY, Lee JH. Korean red ginseng improves glucose control in subjects with impaired fasting glucose, impaired glucose tolerance, or newly diagnosed type 2 diabetes mellitus. *J Med Food* 2014;17(1):128–34.
- Zheng T, Shu G, Yang Z, Mo S, Zhao Y, Mei Z. Antidiabetic effect of total saponins from *Entada phaseoloides* (L.) Merr. in type 2 diabetic rats. *J Ethnopharmacol* 2012;139:814–21.
- Nam KY, Ko SR, Choi KJ. Relationship of saponin and non-saponin for the quality of ginseng. *J Ginseng Res* 1998;22(4):274–83.
- Wang PC, Zhao S, Yang BY, Wang QH, Kuang HX. Anti-diabetic polysaccharides from natural sources: a review. *Carbohydrate Polymers* 2016;148:86–97.
- Zou S, Zhang X, Yao W, Niu Y, Gao X. Structure characterization and hypoglycemic activity of a polysaccharide isolated from the fruit of *Lycium barbarum* L. *Carbohydrate Polymers* 2010;80(4):1161–7.
- Zhang S, Li XZ. Inhibition of α -glucosidase by polysaccharides from the fruit hull of *Camellia oleifera* Abel. *Carbohydrate Polymers* 2015;115:38–43.
- Jiang S, Du P, An L, Yuan G, Sun Z. Anti-diabetic effect of *Coptis chinensis* polysaccharide in high-fat diet with STZ-induced diabetic mice. *International Journal of Biological Macromolecules* 2013;55:118–22.
- Park HJ, Rhee MH, Park KM, Nam KY, Park KH. Effect of non-saponin fraction from *Panax ginseng* on cGMP and thromboxane A2 in human platelet aggregation. *J Ethnopharmacol* 1995;49:157–62.
- Kurimoto H, Nishijo H, Uwano T, Yamaguchi H, Zhong YM, Kawanishi K, Ono T. Effects of nonsaponin fraction of red ginseng on learning deficits in aged rats. *Physiol Behav* 2004;82:345–55.
- Sohn EH, Kim JH, Choi HS, Park HJ, Kim BO, Rhee DK, Pyo SN. Immunomodulatory effects of non-saponin red ginseng components on innate immune cells. *J Ginseng Res* 2008;32(1):67–72.
- Kim EH, Park JD, Pyo SN, Rhee DK. Effects of non-saponin red ginseng components on multi-drug resistance. *J Ginseng Res* 2007;31(2):74–8.
- Lee SH, Park MH, Heo SJ, Kang SM, Ko SC, Han JS, Jeon YJ. Dieckol isolated from *Ecklonia cava* inhibits α -glucosidase and α -amylase in vitro and alleviates postprandial hyperglycemia in streptozotocin-induced diabetic mice. *Food and Chemical Toxicology* 2010;48:2633–7.
- Shan X, Liu X, Hao JJ, Cai C, Fan F, Dun Y, Zha X, Liu X, Li C, Yu G. In vitro and in vivo hypoglycemic effects of brown algal fucoidans. *Int J Biol Macromol* 2016;82:249–55.
- Kasabri V, Affi FU, Hamdan I. In vitro and in vivo acute antihyperglycemic effects of five selected indigenous plants from Jordan used in traditional medicine. *J Ethnopharmacol* 2011;133:888–96.
- Wang Y, Yang Z, Wei X. Sugar compositions, α -glucosidase inhibitory and α -amylase inhibitory activities of polysaccharides from leaves and flowers of *Camellia sinensis* obtained by different extraction methods. *Int J Biol Macromol* 2010;47:534–9.
- Kumar S, Narwal S, Kumar V, Prakash O. α -glucosidase inhibitors from plants: a natural approach to treat diabetes. *Phcog Rev* 2011;5(9):19–29.
- Hamid HA, Yusoff MM, Liu M, Karim MR. α -glucosidase and α -amylase inhibitory constituents of *Tinospora crispa*: isolation and chemical profile confirmation by ultra-high performance liquid chromatography-quadrupole time-of-flight/mass spectrometry. *J Funct Foods* 2015;16:74–80.
- Zuraini A, Zamhuri KF, Yaacob A, Siong CH, Selvarajah M, Ismail A, Hakim MN. *In vitro* anti-diabetic activities and chemical analysis of polypeptide-k and oil isolated from seeds of *Momordica charantia* (Bitter Gourd). *Molecules* 2012;17:9531–640.
- Johnston K, Sharp P, Clifford M, Morgan L. Dietary polyphenols decrease glucose uptake by human intestinal Caco-2 cells. *FEBS Letters* 2005;579: 1653–7.
- Manzano S, Williamson G. Polyphenols and phenolic acids from strawberry and apple decrease glucose uptake and transport by human intestinal Caco-2 cells. *Mol Nutr Food Res* 2010;54:1773–80.
- Kobayashi Y, Suzuki M, Satsu H, Arai S, Hara Y, Suzuki K, Miyamoto Y, Shimizu M. Green tea polyphenols inhibit the sodium-dependent glucose transporter of intestinal epithelial cells by a competitive mechanism. *J Agric Food Chem* 2000;48:5618–23.
- Wang A, Clifford MN, Sharp P. Analysis of chlorogenic acids in beverages prepared from Chinese health foods and investigation, in vitro, of effects on glucose absorption in cultured Caco-2 cells. *Food Chem* 2008;108:369–73.
- Andrade-Cetto A, Vazquez RC. Gluconeogenesis inhibition and phytochemical composition of two *Cercopia* species. *J Ethnopharmacol* 2010;130:93–7.
- Alberti KG, Zimmet PZ. New diagnostic criteria and classification of diabetes-again? *Diabet Med* 1998;7:535–6.
- Zheng W, Welihinda A, Mechanic J, Ding H, Zhu L, Lu Y, Deng Z, Sheng Z, Lv B, Chen Y, et al. EGT1442, a potent and selective SGLT2 inhibitor, attenuates blood glucose and HbA1c levels in db/db mice and prolongs the survival of stroke-prone rats. *Pharmacol Res* 2011;63:284–93.
- Tan KCB, Shiu SWM, Wong Y, Tam X. Serum advanced glycation end products (AGEs) are associated with insulin resistance. *Diabetes Metab Res Rev* 2011;27:488–92.
- Jo R, Min JR, Jeong SH. Anti-diabetic effects of water extracts of *Rehmannia glutinosa* libosch root in 3T3-L1 adipocytes and C57BL/KsJ-db/db mice. *J Korean Soc Food Sci Nutr* 2018;47(10):957–65.
- Klover PJ, Mooney RA. Hepatocytes: critical for glucose homeostasis. *Int J Biochem Cell Biol* 2004;36:753–8.
- Basu A, Basu R, Shah P, Vella A, Johnson CM, Nair KS, Jensen MD, Schwenk WF, Rizza RA. Type 2 diabetes impairs splanchnic uptake of glucose but does not alter intestinal glucose absorption during enteral glucose feeding: additional evidence for a defect in hepatic glucokinase activity. *Diabetes* 2001;50:1351–62.
- Huang X, Liu G, Guo J, Su Z. The PI3K/AKT pathway in obesity and type 2 diabetes. *Int J Biol Sci* 2018;14(11):1483–96.
- Yan F, Zhang J, Zhang L, Zheng X. Mulberry anthocyanin extract regulates glucose metabolism by promotion of glycogen synthesis and reduction of gluconeogenesis in human HepG cell. *Food Funct* 2016;7:425.

- [52] Saini V. Molecular mechanisms of insulin resistance in type 2 diabetes mellitus. *World Journal of Diabetes* 2010;1(3):68–75.
- [53] Padiya R, Chowdhury D, Borkar R, Srinivas R, Bhadra MP, Banerjee SK. Galic attenuates cardiac oxidative stress via activation of PI3K/AKT/Nrf2-Keap1 pathway in fructose-fed diabetic rat. *PLOS ONE* 2014;9(5):e94228.
- [54] Liu TY, Shi CX, Gao R, Sun HJ, Xiong XQ, Ding L, Chen L, Li YH, Wang JJ, Kang YM, et al. Irisin inhibits hepatic gluconeogenesis and increases glycogen synthesis via the PI3K/Akt pathway in type 2 diabetic mice and hepatocytes. *Clinical Science* 2015;129:839–50.
- [55] Granado-Serrano AB, Martin MA, Goya L, Bravo L, Ramos S. Time-course regulation of survival pathways by epicatechin on HepG2 cells. *J Nutr* 2010;103:168–79.
- [56] Martin MA, Granado-Serrano AB, Ramos S, Izquierdo Pulido M, Bravo L, Goya L. Cocoa flavonoids up-regulate antioxidant enzyme activity via the ERK1/2 pathway to protect against oxidative stress-induced apoptosis in HepG2 cells. *J Nutr Biochem* 2010;21:196–205.
- [57] Borradaile NM, de Dreu LE, Huff MW. Inhibition of ne HepG2 cell apolipoprotein B secretion by the citrus flavonoid naringenin involves activation of phosphatidylinositol 3-kinase, independent of insulin receptor substrate-1 phosphorylation. *Diabetes* 2003;52:2554–61.
- [58] Cao H, Hininger-Favier I, Kelly MA, Benaraba R, Dawson HD, Coves S, Roussel AM, Anderson RA. Green tea polyphenol extract regulates the expression of genes involved in glucose uptake and insulin signaling in rats fed a high fructose diet. *J Agric Food Chem* 2007;55:6372–8.
- [59] Nordlie R, Bode AM, Foster JD. Recent advances in hepatic glucose-6-phosphate regulation and function. *Proc Soc Exp Biol Med* 1993;3:274–85.
- [60] Mithieux G. New knowledge regarding glucose-6-phosphatase gene and protein and their roles in the regulation of glucose metabolism. *Eur J Endocrinol* 1997;136:137–45.
- [61] Davies GF, Khandelwal RL, Wu L, Juurlink BH, Roesler WJ. Inhibition of phosphoenolpyruvate carboxykinase (PEPCK) gene expression by troglitazone: a peroxisome proliferators-activated receptor-gamma (PPAR gamma)- independent, antioxidant-related mechanism. *Biochem Pharmacol* 2001;62:1071–9.
- [62] Kim HS, Noh JH, Hong SH, Hwang YC, Yang TY, Lee MS, Kim KW, Lee MK. Rosiglitazone stimulates the release and synthesis of insulin by enhancing GLUT-2, glucokinase and BETA2/NeuroD expression. *Biochem Biophys Res Commun* 2008;367:623–9.
- [63] Ohtsubo K, Takamatsu S, Minowa MT, Yoshida A, Takeuchi M, Marth JD. Dietary and genetic control of glucose transporter 2 glycosylation promotes insulin secretion in suppressing diabetes. *Cell* 2005;123:1307–21.
- [64] Valera A, Solanes G, Fernández-Alvarez J, Pujol A, Ferrer J, Asins G, Gomis R, Bosch F. Expression of GLUT-2 antisense RNA in beta cells of transgenic mice leads to diabetes. *J Biol Chem* 1994;269:28543–6.
- [65] Zhang F, Xu X, Zhang Y, Zhou B, He Z, Zhai Q. Gene expression profile analysis of type 2 diabetic mouse liver. *PLOS ONE* 2013;8(3):e57766.
- [66] Davies SP, Sim AT, Hardie DG. Location and function of three sites phosphorylated on rat acetyl-CoA carboxylase by the AMP-activated protein kinase. *Eur J Biochem* 1990;187:183–90.
- [67] Zhang XD, Yan JW, Yan GR, Sun XY, Ji J, Li YM, Hu YH, Wang HY. Pharmacological inhibition of diacylglycerol acyltransferase 1 reduces body weight gain, hyperlipidemia, and hepatic steatosis in db/db mice. *Acta Pharmacol Sin* 2010;31:1470–7.